REFERENCES

·wal, Y. P., L. R. Sykes, D. W. Simpson and P. G. Richards (1975). Spatial and temporal variations in ts/tp and in P-wave residuals at Blue Mountain Lake, New York: Application to earthquake prediction, Jour. Geophys. Res., 80, 718-732.

›n, A. F. and G. H. Fogle (1974). Intensity survey of Lincoln County, Georgia, McCormick County, South Carolina Earthquake, August 2, 1974, Earthquake Notes, XLV, 4, 27-29.

ıan, J. L., and C. A. von Hake, editors (1973). Earthquake History of the United States (revised edition through 1970), Publication 41-1, Environmental Data Service, NOAA, U.S. Dept. of Commerce, Boulder, Colorado.

, L. T. (1974). Earthquake sequences and b values in the Southeast United States. Bull. Seism. Soc. Am., 64, 267-273.

, L. T. and H. E. Denman (1974). The Georgia-South Carolina earthquake of 2 August 1974; foreshock survey and macroseismic effects, Abstract 46 Annual Meeting, Eastern Section of the Seismological Society of America, Cambridge, Mass.

ɜtreet, W. C. and H. Bell, III (1965). The crystalline rocks of South Carolina, U.S. Geol. Survey Bull. 1186, p. 126.

, M. L., J. Armbruster and Yash Pal Aggarwal (1972). The Adirondack, New York, earthquake swarm of 1971 and tectonic implications, Bull. Seism. Soc. Am. 62, 1303-1318.

ɜni, P., D. T. Secor, V. Montenyohl, P. Scheffler and S. R. Bridges (1974). Aftershock studies following the 2 August 1974 South Carolina earthquake, Abstract 46 Annual Meeting, Eastern Section of the Seismological Society of America, Cambridge, Mass.

VOL. 46, NO. 4 EARTHQUAKE NOTES OCTOBER-DECEMBER 1975

A STUDENT'S GUIDE TO THE USE OF P AND S WAVE DATA FOR FOCAL MECHANISM DETERMINATION

Robert B. Herrmann

CIRES, University of Colorado/NOAA
Boulder, Colorado 80302

ABSTRACT: The purpose of this paper is to serve as an introduction to the use of P and S wave data for the determination of focal mechanisms for those who are not familiar with the mechanics of the process. In particular the determination and plotting of the S-wave polarization angle is discussed in detail. An appendix gives some useful transformations for describing P, SV, and SH amplitudes on the focal sphere in terms of the orientation of the X, Y axes or the P, T axes, or in terms of the strike, dip and slip angles.

INTRODUCTION

The use of P wave first motion data and S wave polarization angles has played an important part in the present understanding of earthquakes. However, the mechanisms of obtaining and using the P and S wave data are sometimes confusing to the student first getting involved with focal mechanisms. Hopefully this paper will serve as an introduction to these studies. This paper will cover the observation and tabulation of data, plotting the data on a stereo net, and interpretation of the plot. An appendix gives theoretical expressions for the far-field P, SV and SH amplitudes.

OBSERVATION AND TABULATION

P Wave First Motion:

a) Read the P wave polarity from the short and long period vertical components for each phase. Ground motion upward is a compression and ground motion downward is a dilatation.

b) Refer to Pho and Behe (1972) for the P wave takeoff angle at the hypocenter, i_h, as a function of epicentral distance and focal depth. For nearby events a local travel time curve can be used to establish such a table. Uncertainty in focal depth for crustal events can lead to differences of up to 10° in the takeoff angle. This uncertainty limits the accuracy of the nodal plane determination.

c) Tabulate the following in a table: station code, epicentral distance, azimuth from epicenter to station, angle of incidence at the source, P phase and P polarity.

S Wave Polarization Data:

a) For crustal events, use observations in the epicentral distance range of 44° to 80°. In this distance range the observed S wave particle motion at the free surface is linear, e.g. the S wave forms on the Z, N and E seismograms are either in phase or 180° out of phase (Nuttli, 1961; Nuttli and Whitemore, 1962). At epicentral distances less than 44°, the vertical, radial and tangential components at the free surface are no longer linear with respect to one another due to the free surface effect (Nuttli, 1961). Mendiguren (1969) was able to use the non-linear particle motion to obtain the polarization angle. Beyond 80°, signal interference arises due to arrivals of ScS, SKS, SP or SKKS close to the S arrival. For the purposes of this paper we restrict our consideration to the epicentral distance range of 44° - 80°. However, this is not a hard and fast rule in that some data may be unusable even in this distance range.

b) If the distance range limitations are satisfied and the observed S wave particle motion is linear, read the relative amplitudes off the three seismograph components, corrected to a common instrument magnification, at the *same instant of time*, as close as possible to the predicted S arrival time.

c) Knowing the back azimuth, θ, the azimuth from the station back to the epicenter, rotate the displacements of the N and E components, U_N and U_E, to form the radial, U_R, and tangential, U_T, components of the S wave motion by the transformation

$$U_R = -\cos\theta\, U_N - \sin\theta\, U_E$$

$$U_T = \sin\theta\, U_N - \cos\theta\, U_E$$

Here U_N and U_E are taken to be positive in the north and east directions, respectively. The U_R component is positive in a direction away from the epicenter, while the U_T component is positive in a direction directed to the right of the ray when viewed from the epicenter towards the station.

d) The S polarization angle, ε, is defined by the relation

$$\tan\varepsilon = U_{SH}/U_{SV}$$

where U_{SH} is the amplitude of the SH component and U_{SV} is the amplitude of the SV component of the S wave. Nuttli (1961) defined U_{SV} as being positive when directed up from the ray in the plane of incidence. This means that U_R and U_Z must be of opposite sign, since U_Z is taken to be positive upward at the receiver. If this is not true, the particular set of S wave data must be used carefully.

Because of the free surface interaction, U_{SV} cannot be measured directly, but Stauder and Bollinger (1964) used the following relation for the polarization angle, ε,

$$\tan\varepsilon = \tan\gamma \cos j_o$$

where $\tan\gamma = (-U_T/U_R)$, with U_T and U_R defined as above, and j_o is the S wave angle of incidence at the free surface. Ignoring the $\cos j_o$ term leads to errors of up to 10 degrees in the determination of ε.

e) From Chandra (1972), obtain the S wave takeoff angle, at the hypocenter, i_h, as a function of focal depth angle epicentral distance.

f) A work sheet for the S data would look like

STA	Δ	AZ	BAZ	Z	N	E	Z	T	R	j_o	ε	i_h
COP	60.0°	311°	79°	0	1	1	0	.8	-1.1	23°	34°	26°
GUA	47.5°	96°	311°	4	11	0	4	-7	-7	26°	-42°	29°

PLOTTING ON A STEREONET

a) It is assumed that the student is familiar with the use of a stereonet. Most seismologists use an equal-area or Lambert-Schmidt projection rather than an equal-angle or Wulff net since the equal-area net provides a less cluttered plot of data whose takeoff angles are less than 45°, which is generally the case. Place tracing paper over the stereonet, mark the center, outline the perimeter, mark north and south.

b) For P waves mark the azimuth, AZ, of the station on the perimeter, rotate the tracing paper about the center of the projection until the tic mark is aligned along an azimuth of 0°, 90°, 180° or 270°. Measure off i_h degrees from the center. This gives the intersection of the particular ray (AZ, i_h) with the focal sphere. Mark the polarity with a small, neat +, for compression, -, for dilatation, or a X, for an indeterminate arrival. These directions are for rays leaving the lower half of the focal sphere. For rays leaving the upper hemisphere, the equivalent lower hemisphere plotting location would be at (AZ + 180°, 180° - i_h).

c) For S wave polarization data, mark the azimuth of the station on the perimeter, rotate the paper so that the station tic falls along an azimuth of 0°, 90°, 180° or 270°. Measure i_h degrees from the center and make a small dot. This point is the intersection of the particular S ray with the focal sphere. Now place this dot at the center of the stereonet and draw a small line making an angle ε with respect to the azimuth of the station. For example, Figure 1 plots the following S wave polarization data.

HERRMANN

STA	AZ	i_h	ϵ
COP	315	45	-30
RAB	90	20	0
AAE	225	30	30

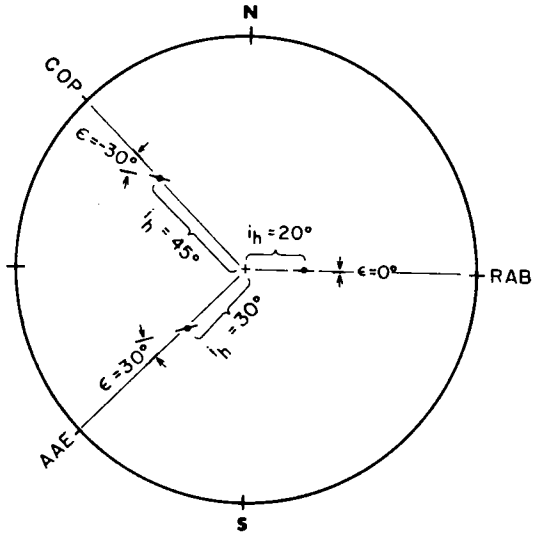

Figure 1. Illustration of the convention for plotting the polarization angle, ϵ.

INTERPRETATION

The double-couple without moment model of the earthquake source is usually used for the interpretation of P and S wave data. The theoretical expressions for the far field displacements due to this source are given in the Appendix.

Some features of this model pertinent to the interpretation of the data obtained by following the outline above are the following.

a) P wave polarities on the focal sphere are such that adjacent quadrants have opposite polarities. These regions are delineated by two perpendicular great circles marking the intersection of the nodal planes

with the focal sphere. A tension axis, T, is located at the center of the compressional quadrant while a pressure axis, P, is located at the center of the dilatational quadrant. Maximum P wave amplitudes occur in the directions of these axes. The P and T axes lie in a plane which is perpendicular to the nodal planes and whose intersection with the focal sphere is also a great circle. The P and T axes are each a distance of 45° from the intersection of the nodal planes with their own great circle. P-wave arrivals with low amplitude or uncertain polarity indicate that the particular ray may be leaving the source near a nodal plane.

b) S wave particle motion is positive in any direction going from the P axis to the T axis. The S wave polarization tics, as plotted above, converge at the T and P axes and are perpendicular to the nodal planes. The orientation of the S wave polarizations is illustrated in Figure 2.

c) The interpretation of the data consists of determining two perpendicular nodal planes which satisfy the P wave polarity data and the S wave polarization data.

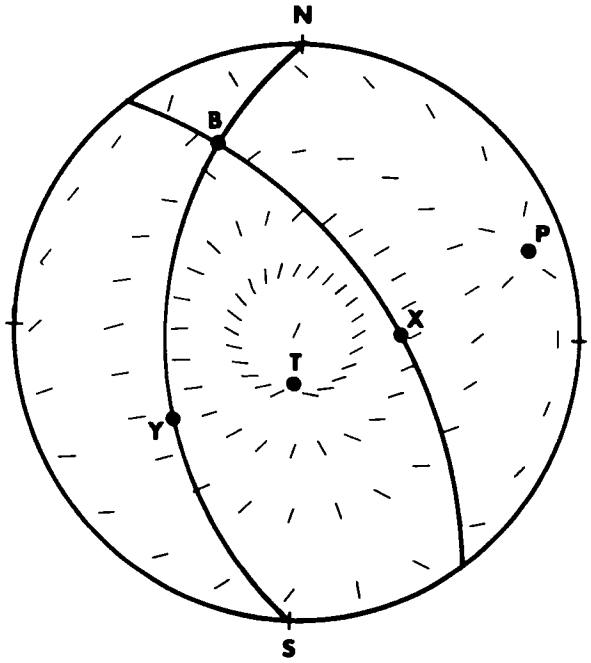

Figure 2. Polarization pattern of S waves showing convergence at P and T axes and perpendicularity with respect to nodal planes.

APPENDIX

Stauder (1960) presented the relations for the far-field P, SV and SH displacements due to a double-couple without moment source in an infinite elastic medium in terms of an x, y, z cartesian coordinate system with an origin at the earthquake focus with the couples acting in the x, y plane. Because the definitions of SH and SV depend upon the coordinate system of the observer, an $\bar{x}$, $\bar{y}$, $\bar{z}$ cartesian system is defined with an origin at the earthquake focus with the $\bar{x}$, $\bar{y}$ and $\bar{z}$ axes directed north, east and down, respectively.

Knowing the orientation of the x, y, z coordinate system with respect to the $\bar{x}$, $\bar{y}$, $\bar{z}$ coordiante system, the far-field body wave amplitudes can be determined for any ray leaving the focal sphere. Let Φ be the azimuth, measured clockwise from north, along which a ray is directed and let i_h be the angle of incidence of the ray at the source measured with respect to the positive z axis ($0° \leq h \leq 180°$).

The $(\bar{x}, \bar{y}, \bar{z})$ coordinates of the intersection of the ray leaving the focus and the focal sphere of radius R are given by

$$\begin{aligned} \bar{x} &= R \sin i_h \cos \Phi \\ \bar{y} &= R \sin i_h \sin \Phi \\ \bar{z} &= R \cos i_h \end{aligned} \qquad \text{A.1}$$

The transformation of an $(\bar{x}, \bar{y}, \bar{z})$ coordinate into an (x, y, z) coordinate is given by the relations

$$\begin{aligned} x &= a_{11}\bar{x} + a_{12}\bar{y} + a_{13}\bar{z} \\ y &= a_{21}\bar{x} + a_{22}\bar{y} + a_{23}\bar{z} \\ z &= a_{31}\bar{x} + a_{32}\bar{y} + a_{33}\bar{z} \end{aligned} \qquad \text{A.2}$$

Defining $R^2 = x^2 + y^2 + x^2$ and following Stauder (1960), the P wave amplitude at a distance R from the source is

$$U_P = \frac{2xy}{4\pi\rho\alpha^3 R^3} K'(t - R/\alpha) \qquad \text{A.3}$$

where α is the compressional wave velocity, ρ the density and K(t) is the time dependence of the couples acting at the source. The prime represents differentiation with respect to the arguments. In terms of dislocation theory

$$K(\infty) = \mu A\bar{u} = M_o$$

where μ is the medium rigidity, A is the area of the dislocation surface, $\bar{u}$ is the average dislocation, and M_o is called the seismic moment. Note that the dependence of the displacement upon distance from the source is on the order of R^{-1}.

The SH displacement is given by the expression

$$U_{SH} = -\frac{1}{4\pi\rho\beta^3} \frac{C}{R^3} K'(t - R/\beta) \qquad \text{A.4}$$

where K is defined as above, β is the transverse wave velocity, and

$$C = (a_{11}y + a_{21}x) \sin \Phi - (a_{12}y + a_{22}x) \cos \Phi$$

The expression for the SV displacement is

$$U_{SV} = \frac{1}{4\pi\rho\beta^3} \frac{D}{R^3} K'(t - R/\beta) \qquad \text{A.5}$$

where

$$D = (2xy \cos i_h - a_{13}y - a_{23}x) / \sin i_h$$

for $\sin i_h \neq 0$ and

$$D = (a_{23}a_{11} + a_{21}a_{13}) \cos \Phi + (a_{12}a_{23} + a_{13}a_{22}) \sin \Phi$$

for the particular case that $\sin i_h = 0$.

We will now define the direction cosines used in equation A.2 in terms of various ways of describing the focal mechanism solution.

1. Given the orientation of the X, Y and Z axes. The X, Y, Z axes form a right handed coordinate system. From equation A.3 it is seen that the nodal planes are the X-Z and Y-Z planes. The Z axis is called the null or B axis. The X, Y and Z axes form a right handed coordinate system with the X and Y axes defined such that P wave compression occurs in the quadrants where the product xy is positive. The orientations of the X, Y, Z axes with respect to the geographic $(\bar{X}, \bar{Y}, \bar{Z})$ coordinate system are usually given in terms of their trend, τ, measured clockwise

from north, and their plunge, π, measured downward from the horizontal. In terms of the trends and plunges of the X, Y and Z axes, the direction cosines of equation A.2 are

$$X = (a_{11},a_{12},a_{13}) = (\cos \tau_x \cos \pi_x, \sin \tau_x \cos \pi_x, \sin \pi_x)$$

$$Y = (a_{21},a_{22},a_{23}) = (\cos \tau_y \cos \pi_y, \sin \tau_y \cos \pi_y, \sin \pi_y)$$

$$Z = (a_{31},a_{32},a_{33}) = (\cos \tau_z \cos \pi_z, \sin \tau_z \cos \pi_z, \sin \pi_z)$$

2. Given the orientation of the P and T axes. The P_T, pressure, and T, tension, axes lie in the X-Y plane at angles of 45° with respect to the X and Y axes.

Vectorially

$$T = \frac{\sqrt{2}}{2}(X + Y) \qquad P = \frac{\sqrt{2}}{2}(X - Y)$$

If τ_P and π_P are the trend and plunge of the P axis and τ_T and π_T are the trend and plunge of the T axis, then

$$X = (a_{11},a_{12},a_{13}) = \frac{\sqrt{2}}{2}(T + P) =$$

$$\frac{\sqrt{2}}{2}(\cos \tau_T \cos \pi_T + \cos \tau_P \cos \pi_P, \sin \tau_T \cos \pi_T + \sin \tau_P \cos \pi_P, \sin \pi_T + \sin \pi_P)$$

and

$$Y = (a_{21},a_{22},a_{23}) = \frac{\sqrt{2}}{2}(T - P) =$$

$$\frac{\sqrt{2}}{2}(\cos \tau_T \cos \pi_T - \cos \tau_P \cos \pi_P, \sin \tau_T \cos \pi_T - \sin \tau_P \cos \pi_P, \sin \pi_T - \sin \pi_P)$$

The use of P and T axes for the description of the focal mechanism is advantageous since there is no confusion as to which quadrants are compressional or dilatational.

3. Given the strike, dip and slip. In sections 2 and 3 we have used four parameters to describe the orientation of the X and Y axes or P and T axes. In fact only three quantities are required to specify the orientation of the double-couple without moment source since the source theory used requires the extra condition that the couples be orthogonal. Thus only three independent parameters need be used to describe the focal mechanism solution.

For these three parameters, we define the motion on the fault plane in terms of the dip, d, and strike, θ, of the fault plane and the angle of slip, s. The relationship of these parameters to the fault plane is shown in Figure A-1. The dip, d, is measured from the horizontal in a downward direction and varies from 0° to 360°. The strike is defined here as the direction of the fault such that the fault plane dips down to the right when looking in the direction of the strike. In other words the hanging wall is to the right when looking along the strike direction. The slip angle gives the direction of motion of the hanging wall with respect to the foot wall; the slip angle varies from -180° to 180°, with the angle of slip positive when measured counterclockwise from the horizontal strike direction. As a way of clarifying the use of the slip angle, slip angles between -180° and 0° have P wave dilatations along the Z axis and slip angles in the range of 0° to 180° have P wave compressions along the Z axis.

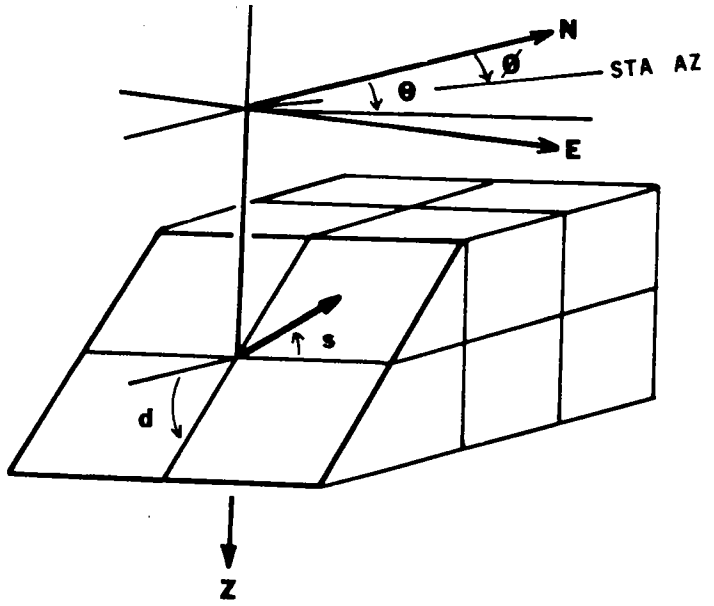

Figure A-1. Representation of fault plane motion in terms of angles of strike, θ, dip, d, and slip, s.

In terms of the strike, θ, dip, d, and slip angle, s, the direction cosines are

$$a_{11} = \cos s \cdot \cos \theta + \sin s \cos d \sin \theta$$

$$a_{12} = \cos s \cdot \sin \theta - \sin s \cos d \cos \theta$$

$$a_{13} = -\sin s \sin d$$

$$a_{21} = -\sin \theta \sin d$$

$$a_{22} = \cos \theta \sin d$$

$$a_{23} = -\cos d$$

$$a_{31} = \cos \theta \sin s - \cos d \cos s \sin \theta$$

$$a_{32} = \cos d \cos \theta \cos s + \sin \theta \sin s$$

$$a_{33} = \cos s \sin d$$

As an illustration of the use of these parameters, the focal mechanism shown in Figure 2 could be described in any of the following manners

$$X = (\tau_x , \pi_x) = (90.0 , 50.0)$$

$$Y = (\tau_y , \pi_y) = (244.6 , 37.2)$$

$$B = (\tau_B , \pi_B) = (344.4 , 12.7)$$

or

$$T = (\tau_T , \pi_T) = (192.7 , 75.6)$$

$$P = (\tau_P , \pi_P) = (75.9 , 6.6)$$

or

$\theta = 180.0°$ $d = 40.0°$ $s = 110.0°$

or

$\theta = 334.6°$ $d = 52.8°$ $s = 74.0°$

ACKNOWLEDGEMENTS

This research was sponsored in part by the Advanced Research Projects Agency of the Department of Defense and was monitored by the Air Force Office of Scientific Research under Grant No. AFOSR-75-2775.

REFERENCES

Chandra, U. (1972). Angles of incidence of S waves, Bull. Seism. Soc. Am. 62, 903-915.

Mendiguren, J. (1969). Study of focal mechanism of deep earthquakes in Argentina using non-linear particle motion and S waves, Bull. Seism. Soc. Am. 59, 1449-1473.

Nuttli, O. W. (1961). The effect of the earth's surface on the S wave particle motion, Bull. Seism. Soc. Am. 51, 237-246.

Nuttli, O. W. and J. D Whitmore (1962). On the determination of the polarization angle of the S wave, Bull. Seism. Soc. Am. 52, 95-107.

Stauder, W. (1960). S waves and focal mechanisms: The state of the question, Bull. Seism. Soc. Am. 50, 333-346.

Stauder, W. and G. A. Bollinger (1964). The S wave project for focal mechanism studies. Earthquakes of 1962, Bull. Seism. Soc. Am. 54, 2199-2208.

Pho, H.-T. and L. Behe (1972). Extended distances and angles of incidence of P waves, Bull. Seism. Soc. Am. 62, 885-902.